ELSEVIER

Journal of Magnetism and Magnetic Materials 213 (2000) 271–277

Journal of magnetism and magnetic materials

www.elsevier.com/locate/jmmm

Low-field magnetic properties of $La_{1-x}Ca_xMnO_3$ ($0 \leqslant x \leqslant 0.4$)

R. Laiho[a,*], K.G. Lisunov[b], E. Lähderanta[a], P. Petrenko[b], V.N. Stamov[b], V.S. Zakhvalinskii[b]

[a] *Wihuri Physical Laboratory, Department of Physics, University of Turku, FIN-20014 Turku, Finland*
[b] *Institute of Applied Physics, Academiei Str. 5, MD-2028 Kishinev, Moldova*

Received 28 August 1999; received in revised form 4 January 2000

Abstract

Magnetic properties of cubic $La_{1-x}Ca_xMnO_3$ ($0 \leqslant x \leqslant 0.4$) are investigated between $T = 5$ and 310 K in the external field of 2 G. The dependence of the ferromagnetic transition temperature on x is analyzed with the model of spin polarons associated with electronic localization and electron–electron interaction. The bandwidth of the localized electrons is found to be $W = 1.90 \pm 0.05$ eV. In the samples with $x < 0.2$ and the Mn^{4+} concentration $c < 0.26$, a transition to a canted antiferromagnetic spin state is observed. The dependence of the transition temperature, T_1, on c can be well described by a model including the Mn^{3+}–Mn^{3+} superexchange and the Mn^{3+}–Mn^{4+} double-exchange interactions. In the samples with $x \leqslant 0.2$ and $c \leqslant 0.22$ the value of the critical exponent, $\gamma = 1.21 \pm 0.05$, is obtained for the temperature dependence of the zero-field-cooled susceptibility function $\chi^{-1}(T) \sim (T - T_C)^{\gamma}$, for $T > T_C$.

PACS: 75.20.C; 75.30.C; 75.30.E

Keywords: Antiferromagnetic materials; Low-field properties; Magnetization; Magnetic compounds

1. Introduction

The undoped manganite $LaMnO_3$ is known as an insulator with antiferromagnetic (AFM) ordering of the Mn^{3+} ions. However, both magnetic and transport properties of this and related manganite and cobaltite perovskites can be substantially varied by hole doping [1]. Namely, if a part of Mn^{3+} ions is changed for Mn^{4+} the compound becomes a mixed valence material, and a new type of interaction (the double exchange) between the Mn ions appears. This may be achieved in two different ways. The first is substitution of Ca^{2+} (or another divalent alkaline element, e.g. Ba, Sr, etc.) for La^{3+} to form alloys like $La_{1-x}Ca_xMnO_3$ (briefly LCMO) [1]. The other way is formation of cation vacancies in the lattice [2,3] or deviations from the ideal oxygen stoichiometry [4]. At high temperatures LCMO is a paramagnet (PM). Its low-temperature magnetic and transport properties are different in different intervals of the Mn^{4+} ion concentration, c. Namely, for $0 \leqslant c < 0.18$ and temperatures $T < T_N$, LCMO is an AFM insulator while for $0.18–0.20 \leqslant c < 0.5$ and $T < T_C$ it is a ferromagnetic (FM) metal, where T_N and T_C are the Néel and the Curie temperature, respectively [1,5].

* Corresponding author.

0304-8853/00/$ - see front matter
PII: S0304-8853(00)00023-8

Near $c \approx 0.5$ ordering of Mn^{3+} and Mn^{4+} ions is observed [6,7]. Additionally, for $c \approx 0.33$ (where T_C attains its maximum) application of an external magnetic field at temperatures near T_C results in a very large decrease of the resistivity. This effect, known as the 'colossal magnetoresistance', has attracted much attention since its very discovery [8].

The magnetic and transport properties of LCMO are believed to be determined by competition between the Mn^{3+}–Mn^{3+} superexchange (SE) interaction, leading to the AFM ordering, and the double-exchange (DE) mechanism aligning the Mn^{3+}–Mn^{4+} spins ferromagnetically by electron transfer via O^{2-} ions [9,10]. Additionally, an interplay of the SE and DE interactions can form below $T_1 < T_N$, T_C a canted AFM orientation of Mn spins [10]. However, the DE mechanism has been criticized for omission of the electron–lattice interaction and association of the Jahn–Teller (JT) effect was suggested [11]. Several theoretical attempts have been made [12,13] to incorporate formation of lattice polarons in perovskite manganites, as a consequence of the JT effect. Different types of magnetic polarons have been introduced, including small polarons (one carrier) [14], large polarons (large amount of carriers) [15] or spin polarons associated to electronic localization [16]. There is evidence, obtained by neutron-scattering experiments, that droplets with magnetic coupling different from the matrix may exist in the FM phase of LCMO [17]. There are also results suggesting that small FM clusters/polarons are present within the PM phase of $La_{0.67}Sr_{0.33}MnO_3$ [18] and in $La_{0.75}Ca_{0.2}Mn(Co)O_3$ [19]. As reported for $La_{0.8}Ca_{0.2}Mn(Co)O_3$ [20], upon approaching T_C from the low-temperature side the FM phase breaks down to small superparamagnetic clusters with size of $\sim$5–10 nm.

As found in many cases, the properties of manganite perovskites depend strongly on the applied magnetic field, B. The external field can (i) expand the FM phase by shifting of T_C towards higher values [5], (ii) influence strongly on the onset of the magnetic irreversibility [21], (iii) cause a coalescence of small spin clusters into larger ones [20] and (iv) destroy the spin canting when B is increased [22]. In this work we investigate the magnetization of LCMO in a field as low as 2 G providing a minimal perturbation of the Mn spin system. The results give important information about magnetic properties of the compound, obtained so far mostly by measurements in much higher fields.

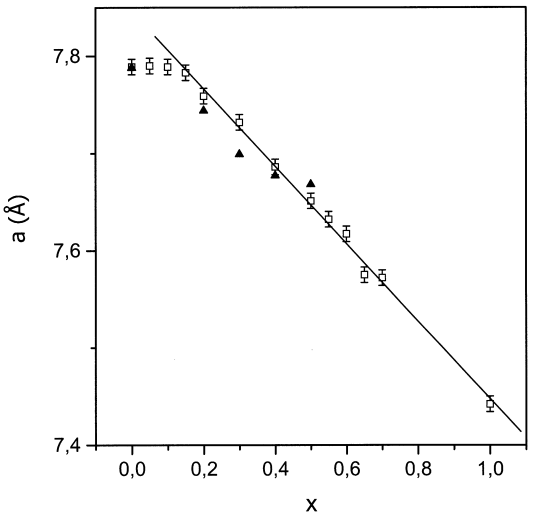

Fig. 1. Dependence of the lattice parameter of $La_{1-x}Ca_xMnO_3$ on the composition. The open symbols represent our data (the solid line is a linear fit for $0.15 \leqslant x \leqslant 1$) and the closed symbols are the data taken from Ref. [2].

2. Experimental results

Samples of LCMO with $0 \leqslant x \leqslant 1$ were synthesized with a standard ceramic technique (see e.g. Ref. [5]) by mixing stoichiometric proportions of La_2O_3, $CaCO_3$ and MnO_2 and heating in air at 1320°C at first for 15 h, then for 5 and 15 h, and at 1375°C for 22 h with intermediate grindings. The X-ray powder diffraction measurements at room temperature showed that all the samples were of single phase, having cubic structure. The dependence of the lattice parameter, a, on composition is shown in Fig. 1 (open symbols). At $0.15 \leqslant x \leqslant 1$ the function $a(x)$ is linear, $a(x) = a_0 - a_1 x$ with $a_0 = 7.846 \pm 0.005$ and $a_1 = 0.399 \pm 0.009$ Å. Additionally, the values of a at corresponding x are close to those found for the cubic LCMO (at $0 \leqslant x \leqslant 0.5$) in Ref. [2] (see Fig. 1, closed symbols).

Table 1
Parameters of the investigated samples (the symbols are explained in the text)

Sample nos.	x	c
#1	0.00	0.21
#2	0.05	0.18
#3	0.15	0.22
#4	0.20	0.26
#5	0.30	0.34
#6	0.40	0.43

DC magnetic measurements were made with a SQUID magnetometer using LCMO samples with $x = 0$, 0.05, 0.15, 0.2, 0.3 and 0.4 (denoted in Table 1 by #1, #2, . . . , #6, respectively). The temperature dependence of the magnetization, $M(T)$, was measured after cooling the samples from 310 to 5 K in zero ($B < 0.1$ G) field (ZFC) or in the field of 2 G (FC). The dependencies of $\chi_{ZFC}(T)$ and $\chi_{FC}(T)$ ($\chi = M/B$) are shown in Fig. 2.

As evident from Fig. 2(a), both $\chi_{ZFC}(T)$ (open symbols) and $\chi_{FC}(T)$ (closed symbols) exhibit a sharp FM transition in samples #2 and #5. Additionally, the plots of $\chi_{ZFC}(T)$ and $\chi_{FC}(T)$ diverge clearly below the magnetic irreversibility temperature $T_i \approx T_C$. The other specimens demonstrate similar magnetic irreversibility. With respect to the dependence of χ_{ZFC} on T the samples can be divided into two groups, displayed separately in Figs. 2(b) and (c). Besides the FM transition at T_C, the samples of the first group with $0 \leqslant x \leqslant 0.15$ (#1–3) exhibit an additional inflection of $\chi_{ZFC}(T)$ at a temperature T_1 between 70 and 100 K. This anomaly is not observed in the samples belonging to the second group with $0.20 \leqslant x \leqslant 0.40$ (#4–6). Behavior of $M(T)$, similar to $\chi_{ZFC}(T)$ for our samples of the first group was recently observed in $La_{0.83}Sr_{0.17}MnO_3$ at $T_1 \approx 128$ K in the field of $B = 100$ G and interpreted as a second magnetic transition (predicted in Ref. [10]) where the Mn moments cant antiferromagnetically [22]. In low fields the corresponding transition has been observed in LCMO with $x = 0.20$ ($B = 100$ G, $T_1 \approx 75$ K) [23] and in $La_{1-x}Sr_xCoO_3$ with $x = 0.20$ ($B = 20$ G, $T_1 \approx 80$ K) [24]. As shown in Fig. 3, in our LCMO samples these transitions are clearly visible, either as a downward (at T_C) or an upward

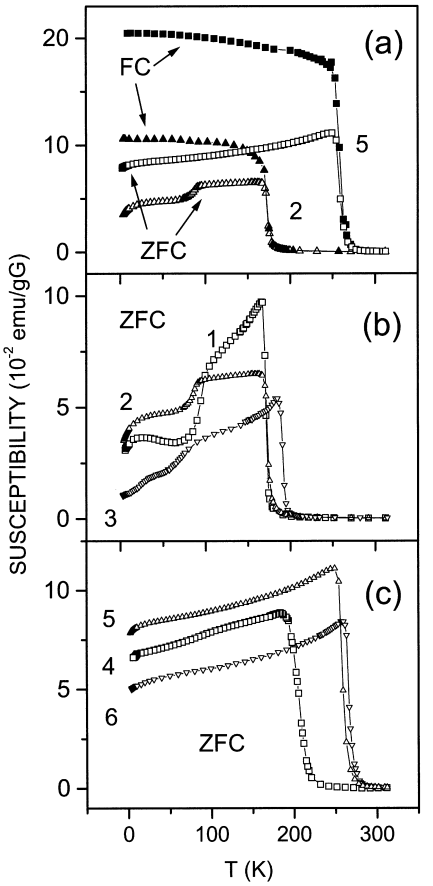

Fig. 2. Temperature dependence of χ_{ZFC} (open symbols) and χ_{FC} (closed symbols) for samples #2 and #5 (a) and of χ_{ZFC} for samples #1–#3 (b) and #4–#6 (c).

(at T_1) peak in the plots of $d\chi_{ZFC}(T)/dT$ versus T. These plots allow accurate determination of the values of T_C and T_1 except for #3 where the peak at T_1 is smeared out.

3. Discussion

To analyze the dependence of T_C on x we apply the model of Varma [16] which treats the PM to FM transition in La manganites by considering the electron localization due to magnetic disorder and the electron–electron interactions. In this model the electrons are localized below the mobility threshold, inside a band with rectangular shape of the

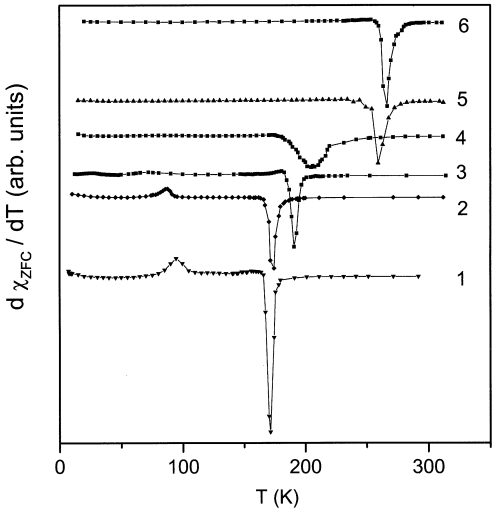

Fig. 3. Dependence of $d\chi_{ZFC}/dT$ on temperature for samples #1–#6.

density of states and the bandwidth W. T_C satisfies the equation

$$T_C \cong 0.1 E_{coh}^F(c), \tag{1}$$

where $E_{coh}^F(c)$ is the electronic cohesive energy in the FM phase,

$$E_{coh}^F(c) = \frac{W}{2} c(1-c). \tag{2}$$

To determine the relation between c and x, we take into account a possibility that cation vacancies (with concentration δ) are generated during preparation of the samples, and that these vacancies can be occupied by Ca^{2+} ions. Each vacancy of the cation sublattice of LCMO yields three Mn^{4+} ions. Therefore, c is increased by one if one Ca^{2+} is substituted for La^{3+}, while c is decreased by two for occupation of a vacancy by Ca^{2+}. The concentration of Mn^{4+} at a given x can be written as $c(x) = c(0) + x_1 + x_2$, where $c(0) = 3\delta$, $x_1 = xP_1(x)$ is the concentration of Ca^{2+} ions substituted for La^{3+} and $x_2 = xP_2(x)$ is the concentration of Ca^{2+} ions which occupy the cation vacancies. Taking into account that the respective probabilities can be written as $P_1(x) = x/(x+\delta)$ and $P_2(x) = \delta/(x+\delta)$, we obtain the concentration

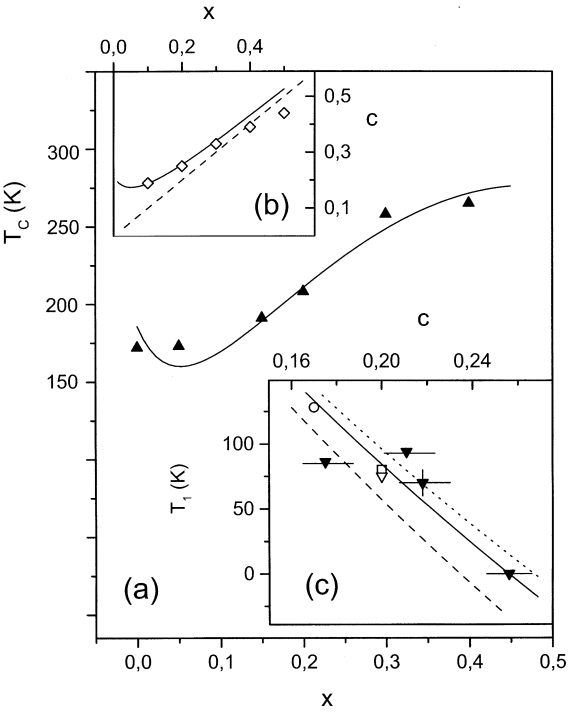

Fig. 4. Experimental dependence of T_C on x (closed symbols) and the fit with Eq. (1) (solid line) (a) dependence of c on x evaluated with Eq. (3) (solid line), the data from Ref. [2] (open symbols) and the concentration of Ca^{2+}, x (dashed line) (b) T_1 versus c obtained in this work (solid symbols) and the data from Refs. [22] (O), [23] (□) and [24] (▽) (c).

of the Mn^{4+} ions as

$$c(x) = \frac{x^2 + \delta x + 3\delta^2}{x + \delta}. \tag{3}$$

The experimental dependence of T_C on x is shown in Fig. 4(a) together with the fit (solid line) calculated with Eqs. (1)–(3), using W and δ as adjustable parameters. A reasonable agreement with the experimental data is obtained for $W = 1.90 \pm 0.05$ eV and $\delta = 0.071 \pm 0.006$. Note that δ should be sensitive to details of the preparation method and can vary randomly from sample to sample. However, as seen from Fig. 4(b) the dependence of c on x evaluated with Eq. (3) (solid line) is in the interval of $0.1 \leqslant x \leqslant 0.3$ very close to that obtained independently in Ref. [2] (open symbols). At low x the calculated dependence deviates

distinctly from the concentration of Ca^{2+} (dashed line), agreeing well with the behavior in Ref. [2]. The bandwidth W in LCMO is similar to that ($W \approx 2.5\,\mathrm{eV}$) in $La_{1-x}Sr_xMnO_3$ [16]. Finally, the values of c calculated for our samples with Eq. (3) are listed in Table 1. All samples satisfy the conditions of the FM region of the magnetic phase diagram (see Section 1). The dependence of T_1 on c is shown in Fig. 4(c) (closed symbols). In this figure displayed also are the corresponding data from Refs. [22–24] (open symbols). We compare them with the function $T_1(c)$ derived by de Gennes [10],

$$T_1 = T_C - \frac{2}{3}\left|\frac{1}{\xi} - \frac{2}{5}\right|\left(4bc + \frac{35}{4}T_C\right), \tag{4}$$

where $\xi = bc/(|J|\,S^2)$, J is the AFM exchange integral of the SE interaction, $S = \frac{3}{2}$ and b is the electron transfer integral which determines the DE coupling. The value of $\beta \equiv b/(|J|S^2) \approx 16$ [10] has been obtained using results of neutron diffraction experiments [1] in LCMO with $x \leqslant 0.2$. From the width of the spin-wave spectrum determined in $LaMnO_3$ by neutron scattering [26], the value of $|J| = 7.2\,\mathrm{K}$ was found, and for $\beta = 16$ the value of $b = 270\,\mathrm{K}$ was obtained [25]. For $CaMnO_3$ a smaller value of $|J| \approx 6.4\,\mathrm{K}$ (due to the difference between the ionic radii of La and Ca) was estimated using $T_N = 90\,\mathrm{K}$ [25].

The values of T_1 shown in Fig. 4(c) were determined for $x \leqslant 0.2$. Using the values of $|J|$ for $LaMnO_3$ and $CaMnO_3$ in Ref. [25], we conclude that the variation of $|J|$ for these values of x is about 2% and can be neglected. The dependence of T_1 on c evaluated with Eq. (4) by taking a slightly higher value of $|J| = 7.7$ and $b = 270\,\mathrm{K}$ is shown in Fig. 4(c) (the solid line). This line reproduces well both the experimental dependence of T_1 on c (the uncertainty of c is shown by the horizontal error bars) and the value of c where the transition to the canted AFM state disappears (shown by the point at $T_1 = 0$ and $c = 0.26$ for #4, see also Fig. 3).

It has been suggested, however, that in doped $LaMnO_3$ b can depend strongly on the average distance between Mn ions, $\langle r_A \rangle$ [27]. Because the parameters c and $\langle r_A \rangle$ are interrelated, this may lead to a corresponding dependence of the transfer integral on c what has not been taken into account above. To estimate possible variation of b with c, we evaluate the function $T_1(c)$ by assuming a linear dependence, $b = b_0 + b_1 c$ with $b_0 = 270\,\mathrm{K}$, $b_1 = -40\,\mathrm{K}$ (Fig. 4(c), dotted line) and $b_1' = 100\,\mathrm{K}$ (Fig. 4(c), dashed line). The area between these two lines covers all the data points taking into account their errors. Then, the upper limit of the relative variation of b satisfies the condition $\Delta b/b < |\Delta b_1|\Delta c/b_0$ where $|\Delta b_1| = b_1' - b_1 = 140\,\mathrm{K}$ and $\Delta c \approx 0.09$ are the variations of b_1 and c, respectively. These values give $\Delta b/b < 5\%$, i.e. also variation of b in the investigated interval of c is negligible. We conclude that the function $T_1(c)$ can be described satisfactorily by the model of de Gennes [10].

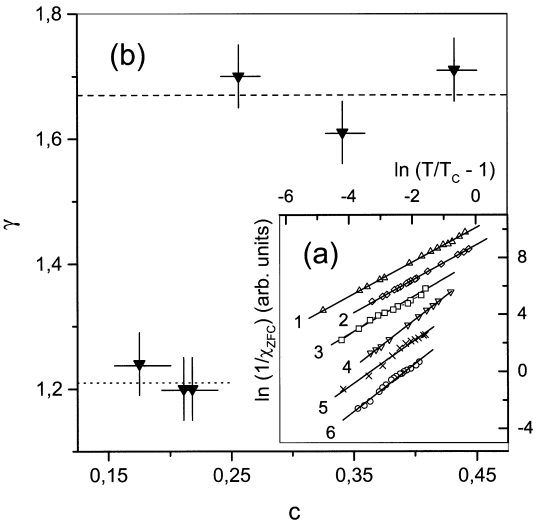

Fig. 5. Dependence of $\ln(1/\chi_{ZFC})$ on $\ln(T/T_C - 1)$ for samples #1–#6 together with linear fits (solid lines) (a). The angular coefficient γ versus c (b).

Finally, we attempt to determine the critical index, γ, of the temperature dependence of the inverse susceptibility near the FM to PM transition ($T > T_C$),

$$\chi^{-1}(T) \propto \left(\frac{T}{T_C} - 1\right)^{\gamma}. \tag{5}$$

The plots of $\ln(1/\chi_{ZFC})$ versus $\ln(T/T_C - 1)$ shown in Fig. 5(a) for samples #1–#6, can be fitted well with a linear function, using the values of the

angular coefficients, γ, presented in Fig. 5(b). The results are quite different for the two groups of the specimens mentioned above: $\gamma = 1.21 \pm 0.05$ for samples #1–3 ($x = 0$–0.15 and $c \approx 0.18$–0.22) and $\gamma^* = 1.67 \pm 0.05$ for samples #4–6 ($x = 0.2$–0.4 and $c \approx 0.26$–0.43).

The values of γ lie between those predicted by the 3D-Heisenberg model ($\gamma = 1.4$) and by the mean-field theory ($\gamma = 1$) [28]. Similar values of γ between these two limits have been found in $La_{0.67}(Ba_yCa_{1-y})_{0.33}MnO_3$ ($\gamma = 1.29$, 1.11 and 1.12 for $y = 1$, 0.5 and 0.25, respectively) from the analysis of modified Arrot plots [29]. A lower value, $\gamma = 1.08$, was obtained in $La_{0.8}Sr_{0.2}MnO_3$ [30], while the values close to that of the 3D-Heisenberg model were determined in $La_{1-x}Sr_xCoO_3$ ($\gamma = 1.39$ for $x = 0.20$, 0.25 and 1.43 for $x = 0.30$) [24].

On one hand, the values of γ^* are similar to those calculated numerically in the percolation theory for 3D case: $\gamma_p = 1.69 \pm 0.05$ [31] and 1.70 ± 0.11 [32]. On the other hand, additional investigations are required to ensure that the parameter γ^* found above for LCMO with $x \geqslant 0.2$ and $c \geqslant 0.26$ really represents the corresponding critical exponent. The point is that from the analysis of the Arrot plots in $La_{0.67}(Ba_yCa_{1-y})_{0.33}MnO_3$ it was established that only in the samples with $y \geqslant 0.25$ the magnetic properties follow the behavior expected for a conventional second-order FM transition [29]. Additionally, in $La_{0.7-y}Pr_yCa_{0.3}MnO_3$ a hysteresis of the temperature dependence of the resistivity, $\rho(T)$, observed near T_C for $y = 0.175$–0.6 demonstrates that in these samples the FM transition is of the first order [27]. However, no hysteresis of $\rho(T)$ can be seen in this compound at $y = 0$ [26]. In the measurements of $\rho(T)$ in LCMO for $0.125 \leqslant x \leqslant 0.5$, the hysteresis was found only for the sample with $x = 0.5$ [23], what is a typical feature of the charge-ordered state. The temperature dependencies of the resistivity, $\rho(T)$ of our LCMO sample #5 with $x = 0.3$ in fields $B = 0, 1, 4$ and 8 T are presented in Fig. 6. The DC measurements performed with the standard four-probe method yield no difference between the curves $\rho(T)$ measured by increasing and decreasing T at any applied field or in any temperature interval between $T = 5$ and 320 K.

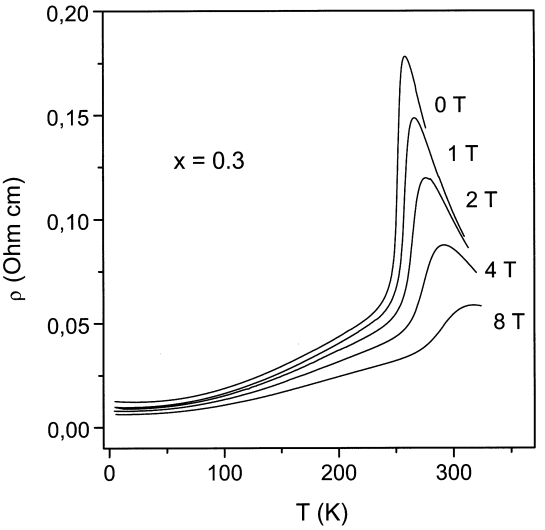

Fig. 6. Temperature dependence of the resistivity for sample #5 with $x = 0.3$ in different magnetic fields.

4. Conclusions

In this work magnetic properties of cubic $La_{1-x}Ca_xMnO_3$ ($0 \leqslant x \leqslant 0.4$) are investigated at T between 5 and 310 K in the magnetic field of 2 G. The analysis of the dependence of the FM Curie temperature, T_C, on x is performed with the model of Varma [16], considering spin polarons associated with electronic localization and electron–electron interactions. The dependence of the concentration of Mn^{4+} on x is obtained by taking into account formation of the vacancies in the cation sublattice of LCMO. At low x the values of c deviate distinctly from the concentration of Ca^{2+} and agree well with those given in Ref. [2]. The value of the bandwidth of the localized electrons, $W = 1.90 \pm 0.05$ eV, is found to be similar to that of $La_{1-x}Sr_xMnO_3$ ($W \approx 2.5$ eV) [16].

In the samples with $x = 0$–0.15 ($c \leqslant 0.22$) a transition to a canted AFM state is observed. The dependence of the transition temperature, T_1, on c agrees satisfactorily with that predicted by the model of de Gennes [10] when the variations of the AFM exchange integral, J, and the electron transfer integral, b, can be neglected.

The value of the critical exponent, $\gamma = 1.21 \pm 0.05$, determined from the slopes of the plots

of ln $(1/\chi_{ZFC})$ versus $\ln(T/T_C - 1)$ for the samples with $x = 0$–0.15 ($c \approx 0.18$–0.22) lies between those of the mean-field theory ($\gamma = 1$) and of the 3D-Heisenberg model ($\gamma = 1.4$). Similar values of γ between these two limits were obtained with the modified Arrot plots for $La_{0.67}(Ba_yCa_{1-y})_{0.33}MnO_3$ with $y \geqslant 0.25$ [29].

The value of the angular coefficient of the dependence of $\ln(1/\chi_{ZFC})$ on $\ln(T/T_C - 1)$, $\gamma^* = 1.67 \pm 0.05$, obtained in the samples with $x = 0.2$–0.4 ($c \approx 0.26$–0.43) is close to the values of the critical exponent, $\gamma_p = 1.69 \pm 0.05$ [31] and 1.70 ± 0.11 [32], calculated in the percolation theory. However, it should be kept in mind that the difference between γ and γ^* may be connected to the possibility of the first-order FM transition in the samples of the second group. In this case γ^* does not present any critical exponent.

References

[1] E.O. Wollan, W.C. Koehler, Phys. Rev. 100 (1955) 545.
[2] R. Mahendrian, S.K. Tiwary, A.K. Raychaudhuri, T.V. Ramakrishnan, R. Mahesh, N. Rangavittal, C.N.R. Rao, Phys. Rev. B 53 (1996) 3348.
[3] S. de Brion, F. Ciorcas, G. Chouteau, P. Lejay, R. Radaelli, C. Chaillout, Phys. Rev. B 59 (1999) 1304.
[4] J. Töpfer, J.B. Goodenough, J. Solid State Chem. 130 (1997) 117.
[5] P. Schiffer, A.P. Ramirez, W. Bao, S.-W. Cheong, Phys. Rev. Lett. 75 (1995) 3336.
[6] C.H. Chen, S.-W. Cheong, Phys. Rev. Lett. 76 (1996) 4042.
[7] M. Roy, J.F. Mitchell, A.P. Ramirez, P. Schiffer, J. Phys.: Condens. Matter 11 (1999) 4843.
[8] R. von Helmolt, J. Wecker, B. Holzapfel, L. Schulz, K. Sammer, Phys. Rev. Lett. 71 (1993) 2331.
[9] C. Zener, Phys. Rev. 82 (1951) 403.
[10] P.-G. de Gennes, Phys. Rev. 118 (1960) 141.
[11] A.J. Millis, P.B. Littlewood, B.I. Shairman, Phys. Rev. Lett. 74 (1995) 5144.
[12] H. Röder, J. Zang, R. Bishop, Phys. Rev. Lett. 76 (1996) 1356.
[13] A.J. Millis, B.J. Shairman, R. Mueller, Phys. Rev. Lett. 76 (1996) 1356.
[14] T. Kasuya, A. Yanase, Rev. Mod. Phys. 40 (1968) 648.
[15] E.L. Nagaev, Phys. Stat. Sol. B 186 (1994) 9.
[16] C.M. Varma, Phys. Rev. B 54 (1996) 7328.
[17] M. Hennion, F. Moussa, G. Biotteau, J. Rodriguez-Carvajal, L. Piusard, A. Revcolevschi, Phys. Rev. Lett. 81 (1998) 1957.
[18] J.W. Lynn, R.W. Ervin, J.A. Borchers, Q. Huang, A. Santoro, J.-L. Peng, Z.Y. Li, Phys. Rev. Lett. 76 (1996) 4046.
[19] M. Pissas, G. Kallias, E. Devlin, A. Simopoulos, D. Niarchos, J. Appl. Phys. 81 (1997) 5770.
[20] V. Chechersky, A. Nath, I. Isaac, J.P. Franck, K. Ghosh, H. Ju, R.L. Greene, Phys. Rev. B 59 (1999) 497.
[21] X.-G. Li, X.J. Fan, G. Ji, W.B. Wu, K.H. Wong, C.L. Choy, H.C. Ku, J. Appl. Phys. 85 (1999) 1663.
[22] J.J. Neumeier, K. Andres, K.J. McClellan, Phys. Rev. B 59 (1999) 1701.
[23] J. Dlo, I. Kim, S. Lee, K.H. Kim, H.J. Lee, J.H. Jung, T.W. Noh, Phys. Rev. B 59 (1999) 492.
[24] J. Mira, J. Rivas, M. Vazques, J.M. Garcia-Beneyetz, J. Arcas, R.D. Sanchez, M.A. Senaris-Rodriguez, Phys. Rev. B 59 (1999) 123.
[25] C.M. Srivastava, J. Phys.: Condens. Matter 11 (1999) 4539.
[26] K. Hiroto, N. Kaneto, A. Nishizawa, E. Endo, J. Phys. Soc. Japan 65 (1996) 3736.
[27] H.Y. Hwang, S.-W. Cheong, P.G. Radaelli, M. Marezio, B. Batlogg, Phys. Rev. Lett. 75 (1995) 914.
[28] H.E. Staney, Introduction to Phase Transitions and Critical Phenomena, Clarendon Press, Oxford, 1971.
[29] N. Moutis, I. Panagiotopulos, M. Pissas, D. Niarchos, Phys. Rev. B 59 (1999) 1129.
[30] Ch.V. Mohan, M. Seeger, H. Kronmuller, P. Murugaraj, J. Maier, J. Magn. Magn. Mater. 183 (1998) 348.
[31] M.F. Sykes, J.W. Essam, Phys. Rev. 133 (1964) 310.
[32] A.G. Dunn, J.W. Essam, D.S. Ritchie, J. Phys. C 8 (1975) 4219.